Generalizing the Fermi velocity of strained graphene from uniform to nonuniform strain

M. Oliva-Leyva [a,*], Gerardo G. Naumis [a,b]

[a] *Departamento de Física-Química, Instituto de Física, Universidad Nacional Autónoma de México (UNAM), Apartado Postal 20-364, 01000 México, Distrito Federal, Mexico*
[b] *School of Physics Astronomy and Computational Sciences, George Mason University, Fairfax, VA 22030, USA*

A B S T R A C T

The relevance of the strain-induced Dirac point shift to obtain the appropriate anisotropic Fermi velocity of strained graphene is demonstrated. Then a critical revision of the available effective Dirac Hamiltonians is made by studying in detail the limiting case of a uniform strain. An effective Dirac Hamiltonian for nonuniform strain is thus reported, which takes into account all strain-induced effects: changes in the nearest-neighbor hopping parameters, the reciprocal lattice deformation and the true shift of the Dirac point. Pseudomagnetic fields are thus explained by means of position-dependent Dirac cones, whereas complex gauge fields appear as a consequence of a position-dependent Fermi velocity. Also, position-dependent Fermi velocity effects on the spinor wavefunction are considered for interesting cases of deformations such as flexural modes.

© 2015 Elsevier B.V. All rights reserved.

1. Introduction

Since its discovery [1], graphene has been subject of many theoretical and experimental studies due to the unique array of its physical properties [2,3]. In particular, the peculiar relation between its electronic and its mechanical properties has attracted growing interest [4–7]. The unusual long interval of elastic response [8] makes it possible observable changes in the electronic structure, such as the opening of a bandgap [9,10] or the merging of Dirac cones [11,12]. The strategy is to use strain engineering as a possibility to guide the electrical transport in graphene-based devices [13–17].

In the literature there are different theoretical approaches for studying the influence of lattice deformations over the electronic properties of graphene. A quantum field theoretical approach in curved spaces has been alternatively used to predict electronic implications due to out-of-plane deformations [18–20]. Also, methods based solely on symmetry considerations have been applied to several problems of strained graphene [21–24]. In particular, using group theory techniques, a symmetry analysis has been performed to construct all the possible terms in the low-energy effective Hamiltonian for graphene in presence of a nonuniform strain [24]. More recently, a formulation based on concepts from discrete differential geometry has shown how the atomistic structure of two-dimensional crystalline membranes dictates their mechanical, electronic, and chemical properties [25–28]. Some particular analytical results are available for the case of uniaxial strain. For periodic strain, a complex fractal spectrum with gaps, localization transitions and topological states are obtained [29].

Nevertheless, the most popular theoretical framework for exploring the concept of strain engineering combines a nearest-neighbor tight-binding (TB) model and linear elasticity theory [4,5]. As is well known, this TB-elasticity approach, in the continuum limit, predicts the existence of strain-induced pseudomagnetic fields. These pseudomagnetic fields are described by means of a pseudovector potential $\boldsymbol{A}$ which is related to the strain tensor $\bar{\epsilon}$ by [5]

$$A_x = \frac{\beta}{2a}(\bar{\epsilon}_{xx} - \bar{\epsilon}_{yy}), \quad A_y = -\frac{\beta}{2a}(2\bar{\epsilon}_{xy}), \tag{1}$$

where a is the unstrained carbon–carbon distance and β is the electron Grüneisen parameter. Thus, nonuniform local deformations of the lattice can be interpreted as a pseudomagnetic field, given by $\boldsymbol{B} = \nabla \times \boldsymbol{A}$ (in units of $\hbar/e$) and perpendicular to the graphene sample [30–34]. Scanning tunneling microscopy studies in graphene nanobubbles have reported pseudo Landau levels, which are signatures of strain-induced pseudomagnetic fields [35,36].

A discussion on the pseudomagnetic field theory was reactivated due to the explicit inclusion of the local lattice vectors de-

formation [37]. Initially, this lattice correction was supposed to produce an extra pseudovector potential ($\boldsymbol{K}_0$-dependent), but later on it was shown its physical irrelevance [38–40]. Particularly, in Ref. [26] the absence of the extra pseudovector potential proposed in the theory was demonstrated in an explicit manner. Also, the consideration of the actual atomic positions in the TB Hamiltonian resulted in a more complete analysis on the position-dependent Fermi velocity for strained graphene [39]. More recently, another correction has been identified as important in the derivation of the effective low-energy Hamiltonian for deformed graphene, by pointing out that the effective Hamiltonian should be expanded around the true Dirac point and not around the unperturbed one [41–44].

The principal motivation of the present work is to determine the implications of the strain-induced Dirac point shift in the derivation of the appropriate anisotropic Fermi velocity. Moreover, we discuss a possible generalization of the effective Dirac Hamiltonian for nonuniform in-plane deformations. For that end, we lay out our discussion on a basic principle: *the theory for graphene under nonuniform strain should describe the particular case of a uniform strain.*

The paper is organized as follows. In Section 2 we discuss the effective Dirac Hamiltonian for graphene under a uniform in-plane strain. By comparing with other approaches available in the literature, we demonstrate the relevance of the expansion around of the true Dirac point. In Section 3 we report a generalized effective Dirac Hamiltonian for graphene under a nonuniform in-plane strain, which reproduces the case of a uniform strain. In Section 4 we summarize the results of our work.

2. Dirac equation for uniformly strained graphene: critical revision

To illustrate the derivation of the effective Dirac Hamiltonian in presence of strain, we first consider graphene under a uniform strain. We use this particular case as a benchmark to identify the goodness of any effective Dirac Hamiltonian for strained graphene, even if the deformation is nonuniform. In the case of a uniform strain, if $\boldsymbol{a}$ represents a general vector in the unstrained graphene lattice, its strained counterpart is given by the transformation

$$\boldsymbol{a}' = (\bar{\boldsymbol{I}} + \bar{\boldsymbol{\epsilon}}) \cdot \boldsymbol{a}, \qquad (2)$$

where $\bar{\boldsymbol{I}}$ is the 2×2 identity matrix and $\bar{\boldsymbol{\epsilon}}$ is the position-independent strain tensor. As an import example, one can quote the deformation of the three nearest-neighbor vectors. Selecting the x axis along the graphene zigzag direction, the unstrained nearest-neighbor vectors are,

$$\boldsymbol{\delta}_1 = \frac{a}{2}(\sqrt{3}, 1), \quad \boldsymbol{\delta}_2 = \frac{a}{2}(-\sqrt{3}, 1), \quad \boldsymbol{\delta}_3 = a(0, -1), \qquad (3)$$

whereas the strained nearest-neighbor vectors can be obtained from $\boldsymbol{\delta}_n' = (\bar{\boldsymbol{I}} + \bar{\boldsymbol{\epsilon}}) \cdot \boldsymbol{\delta}_n$, see Fig. 1(a).

On the other hand, a uniform strain distorts the reciprocal space as well. From Eq. (2) follows that if $\boldsymbol{b}$ represents a vector of the unstrained reciprocal lattice, its deformed counterpart results $\boldsymbol{b}' = (\bar{\boldsymbol{I}} + \bar{\boldsymbol{\epsilon}})^{-1} \cdot \boldsymbol{b} \simeq (\bar{\boldsymbol{I}} - \bar{\boldsymbol{\epsilon}}) \cdot \boldsymbol{b}$ (see Fig. 1(b)). However, the high-symmetry points of the Brillouin zone are modified differently. For example, the high-symmetry point of the unstrained Brillouin zone $\boldsymbol{K}_0 = (\frac{4\pi}{3\sqrt{3}a}, 0)$ moves to the new position $\boldsymbol{K} = \frac{4\pi}{3\sqrt{3}a}(1 - \bar{\epsilon}_{xx}/2 - \bar{\epsilon}_{yy}/2, -2\bar{\epsilon}_{xy})$ under a uniform strain [9].

For computing the effective Dirac Hamiltonian we start from the nearest-neighbor TB Hamiltonian,

$$H = -\sum_{\boldsymbol{x}',n} t_n' a_{\boldsymbol{x}'}^\dagger b_{\boldsymbol{x}'+\boldsymbol{\delta}_n'} + \text{H.c.}, \qquad (4)$$
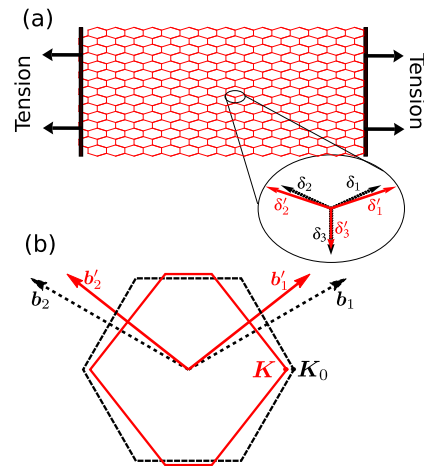
Fig. 1. (Color online.) (a) Uniaxial stretching along the zigzag direction of a graphene sample. The zoom of the honeycomb lattice shows the unstrained $\boldsymbol{\delta}_i$ (black, dashed) and strained $\boldsymbol{\delta}_i'$ (red, solid) three nearest-neighbor vectors. (b) Unstrained (black, dashed) and strained (red, solid) first Brillouin zone for the same uniaxial zigzag strain. Note how the reciprocal lattice is contracted along the direction where the lattice is stretched.

where $\boldsymbol{x}'$ runs over all sites of the deformed A sublattice, $a_{\boldsymbol{x}'}^\dagger$ is the creation operator for an electron on the A sublattice at site $\boldsymbol{x}'$ and $b_{\boldsymbol{x}'+\boldsymbol{\delta}_n'}$ is the annihilation operator for an electron on the B sublattice at site $\boldsymbol{x}' + \boldsymbol{\delta}_n'$. The nearest-neighbor hopping parameters t_n' are modified due to the changes in intercarbon distance and fulfill an exponential decay, $t_n' = t \exp[-\beta(|\boldsymbol{\delta}_n'|/a - 1)]$, where t is the equilibrium hopping parameter [4,45].

Replacing the creation/annihilation operators with their Fourier expansions [46], we obtain that the Hamiltonian in momentum space is given by

$$H = -\sum_{\boldsymbol{k},n} t_n' e^{-i\boldsymbol{k}\cdot(\bar{\boldsymbol{I}}+\bar{\boldsymbol{\epsilon}})\cdot\boldsymbol{\delta}_n} a_{\boldsymbol{k}}^\dagger b_{\boldsymbol{k}} + \text{H.c.}, \qquad (5)$$

and therefore, the closed dispersion relation for uniformly strained graphene is

$$E(\boldsymbol{k}) = \pm \left| \sum_n t_n' e^{-i\boldsymbol{k}\cdot(\bar{\boldsymbol{I}}+\bar{\boldsymbol{\epsilon}})\cdot\boldsymbol{\delta}_n} \right|. \qquad (6)$$

As has been documented in other works [9,42], the positions of the minimum of energy, i.e., the $\boldsymbol{K}_D$ Dirac points ($E(\boldsymbol{K}_D) = 0$) obtained from the previous equation, do not coincide with the $\boldsymbol{K}$ ($\boldsymbol{K}_0$) high-symmetry points of the strained (unstrained) Brillouin zone. This is illustrated in Fig. 2.

Eqs. (5) and (6) are the main ingredients of the available effective Dirac Hamiltonians. As we will discuss below, the main differences come out from the reciprocal-space points used for the approximations. This is also illustrated in Fig. 2, where the idea is to understand how the Dirac cone moves and deforms as strain is applied.

To be more precise, if one considers momenta close to the arbitrary reciprocal-space point $\boldsymbol{G}$, i.e. $\boldsymbol{k} = \boldsymbol{G} + \boldsymbol{q}$, the Hamiltonian (5) can be casted as

$$H_{\boldsymbol{G}} = -\sum_{n=1}^3 t_n' \begin{pmatrix} 0 & e^{-i(\boldsymbol{G}+\boldsymbol{q})\cdot(\bar{\boldsymbol{I}}+\bar{\boldsymbol{\epsilon}})\cdot\boldsymbol{\delta}_n} \\ e^{i(\boldsymbol{G}+\boldsymbol{q})\cdot(\bar{\boldsymbol{I}}+\bar{\boldsymbol{\epsilon}})\cdot\boldsymbol{\delta}_n} & 0 \end{pmatrix}, \qquad (7)$$

and expanding to first order in $\boldsymbol{q}$ and $\bar{\boldsymbol{\epsilon}}$, *as will be used throughout the rest of the paper*, we obtain
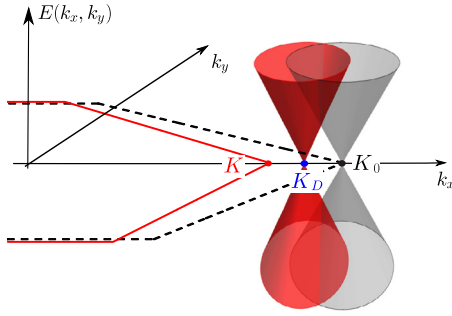
Fig. 2. (Color online.) Sketch of the Dirac cone (red cone) movement as graphene is stretched along the zigzag direction. Three important points are indicated in the reciprocal space, the original Dirac point K_0, the high-symmetry point K of the strained reciprocal lattice and the true Dirac point K_D. The gray Dirac cone is the image of the red Dirac cone for unstrained graphene. The unstrained reciprocal lattice is pictured with black dots.

$$H_G \simeq -\sum_{n=1}^{3} t'_n \begin{pmatrix} 0 & e^{-i G \cdot \delta_n} \\ e^{i G \cdot \delta_n} & 0 \end{pmatrix} (1 + i\sigma_z q \cdot (\bar{I} + \bar{\epsilon}) \cdot \delta_n)$$
$$\times (1 + i\sigma_z G \cdot \bar{\epsilon} \cdot \delta_n), \tag{8}$$

with σ_z being the diagonal Pauli matrix. In the literature, one can find two kinds of expansions by making $G = K_0$ or $G = K_D$. This leads to two different effective Dirac Hamiltonians, as will be discussed in the following subsections.

It is worth mentioning that such Hamiltonians are in fact trying to describe the deformation and movement of the Dirac cone from different points, as explained in Fig. 2. Clearly, if one chooses a point which is not the true Dirac point of the strained system, the Hamiltonian will not display the proper symmetries associated with it. Furthermore, *one cannot pass from one Hamiltonian to the other by using a simple renormalization of the momentum since the Taylor expansions used around each point are different.* The Fermi velocity will be used to test these ideas.

2.1. Effective Hamiltonian around K_0

The most popular expansion in the literature is to consider momenta close to the high-symmetry points of the unstrained Brillouin zone, $G = K_0$ [38–40]. In this case, Hamiltonian (8) can be written as

$$H_{K_0} \simeq -\sum_{n=1}^{3} t'_n \begin{pmatrix} 0 & e^{-i K_0 \cdot \delta_n} \\ e^{i K_0 \cdot \delta_n} & 0 \end{pmatrix} (1 + i\sigma_z q \cdot (\bar{I} + \bar{\epsilon}) \cdot \delta_n)$$
$$\times (1 + i\sigma_z K_0 \cdot \bar{\epsilon} \cdot \delta_n). \tag{9}$$

Using the following identity [20,39]

$$\begin{pmatrix} 0 & e^{-i K_0 \cdot \delta_n} \\ e^{i K_0 \cdot \delta_n} & 0 \end{pmatrix} = i \frac{\sigma \cdot \delta_n}{a} \sigma_z, \tag{10}$$

where $\sigma = (\sigma_x, \sigma_y)$ are the non-diagonal Pauli matrices, and writing the three nearest-neighbor hopping parameters t'_n as

$$t'_n \simeq t \left(1 - \frac{\beta}{a^2} \delta_n \cdot \bar{\epsilon} \cdot \delta_n \right), \tag{11}$$

the Hamiltonian (9) becomes (see Appendix A)

$$H_{K_0} \simeq \hbar v_F \sigma \cdot \left(\bar{I} + \bar{\epsilon} - \frac{\beta}{4}(2\bar{\epsilon} + \mathrm{Tr}(\bar{\epsilon})\bar{I})\right) \cdot q - \hbar v_F \sigma \cdot A$$
$$+ \hbar v_F \sigma \cdot (\frac{a}{2} K_0 \cdot \bar{\epsilon} \cdot \sigma') \cdot q + \hbar v_F \sigma \cdot \bar{\epsilon} \cdot K_0, \tag{12}$$

where $v_F = 3ta/2\hbar$ is the Fermi velocity for unstrained graphene and $\sigma' = (-\sigma_z, \sigma_x)$. Here the A vector is given by Eq. (1) and

as mentioned, is interpreted as a pseudomagnetic vector potential when the strain is nonuniform. It is worth pointing out that the expression (1) was derived by taking the x axis parallel to the zigzag direction of the graphene lattice and considering a valley (K_0) with index $+1$. In the following, we assume these conditions, unless stated otherwise.

Hamiltonian H_{K_0} contains a problem that is very easy to spot. Let us consider a simple isotropic stretching of the lattice, which can be written as $\bar{\epsilon} = \epsilon \bar{I}$. This strain is just a renormalization of the distance between carbons. As a result, the new carbon–carbon distance under isotropic strain is $a' = a(1 + \epsilon)$ and the new hopping parameter to first order in strain is $t' = t(1 - \beta\epsilon)$. Thus, the new Fermi velocity obtained straight away from the nearest-neighbor TB Hamiltonian is $v'_F = 3t'a'/2\hbar \simeq v_F(1 - \beta\epsilon + \epsilon)$ and therefore, the effective Dirac Hamiltonian is $\hbar v'_F \sigma \cdot q$, which cannot be obtained from Eq. (12) to an isotropic strain. This trivial test confirms that H_{K_0} is not appropriate to describe graphene under a uniform strain. Consequently, expansions around the high-symmetry points of the unstrained Brillouin zone lead to unsuitable effective Hamiltonians for strained graphene [44].

2.2. Effective Dirac Hamiltonian around K_D

A second option is to derive an effective Dirac Hamiltonian by expanding (5) around the true Dirac points [41,42,44]. In other words, to make $G = K_D$. As reported in previous work [42], the actual positions of the K_D Dirac points to the K_0 point is given by

$$K_D \simeq (\bar{I} + \bar{\epsilon})^{-1} \cdot K_0 + A, \tag{13}$$

as shown in Fig. 2. The previous equation confirms the remark that K_D coincides with K only for isotropic strain.

Using Eq. (13) it is possible to obtain the proper effective Dirac Hamiltonian by developing Eq. (5) around the Dirac points, $k = K_D + q$. Following this approach one can derive that [42]

$$H = \hbar v_F \sigma \cdot (\bar{I} + \bar{\epsilon} - \beta\bar{\epsilon}) \cdot q, \tag{14}$$

where two strain-induced contributions can be recognized. The β-independent term, $\hbar v_F \sigma \cdot \bar{\epsilon} \cdot q$, is purely a geometric consequence due to lattice deformation and does not depend of the material as long as it has the same topology. On the other hand, the β-dependent term, $-\hbar v_F \beta\sigma \cdot \bar{\epsilon} \cdot q$, is owing to the strain-induced changes in the hopping parameters and its contribution depends of the material since β varies depending on the material. For graphene, both contributions have the same order of magnitude.

From Eq. (14) one can identify that the appropriate Fermi velocity tensor is given by

$$\bar{v} = v_F(\bar{I} + \bar{\epsilon} - \beta\bar{\epsilon}), \tag{15}$$

which consistently reproduces the anisotropic transport for uniformly strained graphene [47,48]. For example, Eq. (15) yields the correct result $v_F(1 - \beta\epsilon + \epsilon)\bar{I}$ when the strain is isotropic, $\bar{\epsilon} = \epsilon\bar{I}$. Also, for the case of an uniaxial stretching,

$$\bar{\epsilon} = \epsilon \begin{pmatrix} 1 & 0 \\ 0 & -\nu \end{pmatrix}, \tag{16}$$

with ν being the Poisson ratio, from Eq. (15) one immediately obtains the known result [9,49]

$$\bar{v} = v_F \begin{pmatrix} 1 + (1-\beta)\epsilon & 0 \\ 0 & 1 - (1-\beta)\epsilon\nu \end{pmatrix}, \tag{17}$$

for the anisotropic Fermi velocity. This expression has been used to calculate and explain the experimentally observed modulation of the transmittance of strained graphene with respect to the polarization direction of the incoming light [49–51].

3. Generalized Dirac Hamiltonian for nonuniformly strained graphene

As mentioned in Section 1, we base our discussion for nonuniformly strained graphene on the following basic principle: *the theory for graphene under nonuniform strain must describe the particular case of a uniform strain*. Therefore, one would expect that the effective Dirac Hamiltonian for nonuniformly strained graphene should reduce to the effective Dirac Hamiltonian for the case of a spatially uniform strain. However, none of the effective Dirac Hamiltonian reported in the literature for the case of a nonuniform strain reduce to Eq. (14). This is an inconsistency in the theory of the strain-induced pseudomagnetic field, which is owing to expansions around points which are not the true Dirac points for strained graphene. Below, we give a proposal to solve the problem.

Unlike the case of uniform strain, a nonuniform strain breaks the crystal periodicity. This delicate issue depends upon the physical considered limit. For example, if the strain is periodic but with a wavelength comparable to the interatomic displacement, in certain cases one needs an infinite number of reciprocal vetors to build the wavefunction, so the present approach cannot be made [29]. Here we will assume that the strain modulation wavelength is much bigger than the interatomic distance, as well as the amplitude. Under such approximation, the problem is usually solved by starting from the uniform Hamiltonian and changing $\bar{\epsilon}$ to $\bar{\epsilon}(\mathbf{r})$.

The problem lies in the fact that now the Fermi velocity $\bar{\mathbf{v}}(\mathbf{r})$ depends upon the position, and thus the term $\bar{v}_{ij}q_k$ breaks the hermiticity of resulting Hamiltonian. To assure hermiticity, the procedure made in previous works to generalize the Dirac Hamiltonian around the *unstrained Dirac point* $\mathbf{K}_0$, using the replacement [20, 39–41],

$$\bar{v}_{ij}q_k \to \bar{v}_{ij}(\mathbf{r})\left(-i\frac{\partial}{\partial r_k}\right) - \frac{i}{2}\frac{\partial \bar{v}_{ij}(\mathbf{r})}{\partial r_k}. \tag{18}$$

However, as we discussed previously, the strain-induced Dirac point shift must be considered in the derivation of the appropriate Fermi velocity. This issue can be solved by starting from the uniform Hamiltonian around the true Dirac point in the momentum space, and going to real space by means of the replacement [44]

$$\bar{v}_{ij}q_k \to \bar{v}_{ij}(\mathbf{r})\left(-i\frac{\partial}{\partial r_k} - K_k^D(\mathbf{r})\right) - \frac{i}{2}\frac{\partial \bar{v}_{ij}(\mathbf{r})}{\partial r_k}, \tag{19}$$

where now we have introduced the explicit position-dependence of the Dirac point by denoting it as $K_k^D(\mathbf{r})$. This approach corresponds to the general scheme of emergence of gravity and gauge fields in the vicinity of the Weyl, Dirac or Majorana points in the energy spectrum [52–54].

Thus, according to Eq. (19) and taking into consideration local rotations (see Appendix B), the effective Dirac Hamiltonian for nonuniform in-plane strain can be written as

$$H = \hbar\boldsymbol{\sigma} \cdot \bar{\mathbf{v}}(\mathbf{r}) \cdot (-i\nabla - \mathbf{K}_D(\mathbf{r})) - \hbar v_F \boldsymbol{\sigma} \cdot \boldsymbol{\Gamma}, \tag{20}$$

where the position-dependent Fermi velocity tensor $\bar{\mathbf{v}}(\mathbf{r})$ is given by

$$\bar{\mathbf{v}}(\mathbf{r}) = v_F\left(\bar{\mathbf{I}} + \bar{\epsilon}(\mathbf{r}) - \beta\bar{\epsilon}(\mathbf{r})\right), \tag{21}$$

the Dirac point $\mathbf{K}_D(\mathbf{r})$ by,

$$\mathbf{K}_D(\mathbf{r}) = \left(\bar{\mathbf{I}} - \bar{\epsilon}(\mathbf{r}) + \bar{\omega}(\mathbf{r})\right) \cdot \mathbf{K}_0 + \mathbf{A}(\mathbf{r}), \tag{22}$$

and the vector field $\boldsymbol{\Gamma}$ as

$$\Gamma_i = \frac{i}{2v_F}\frac{\partial \bar{v}_{ij}(\mathbf{r})}{\partial r_j} = \frac{i(1-\beta)}{2}\frac{\partial \bar{\epsilon}_{ij}(\mathbf{r})}{\partial r_j}, \tag{23}$$

with an implicit sum over repeated indices.

Let us make some important remarks about our effective Hamiltonian (20). First of all, one can see that Eq. (20) reproduces the limiting case of a uniform strain in a consistent manner. This is the principal merit of Hamiltonian (20) with respect to previous effective Hamiltonians. At the same time, one can recognize a new position-dependent Fermi velocity tensor (Eq. (21)) as the main difference. This is a very important result because enables a more appropriate prediction of spatially-varying Fermi velocity. Nowadays, such effect of strain has been confirmed by experiments using scanning tunneling microscopy and spectroscopy [55,56].

In the approach carried out, the position-dependent Dirac point generates the pseudomagnetic fields. This fact can be seen by taking the rotational of the effective potential that appears in Eq. (20) which leads to the pseudomagnetic field,

$$\mathbf{B} = \nabla \times \mathbf{K}_D(\mathbf{r}), \tag{24}$$

but since $\nabla \times ((\bar{\epsilon}(\mathbf{r}) - \bar{\omega}(\mathbf{r})) \cdot \mathbf{K}_0) = 0$, the term $(\bar{\epsilon}(\mathbf{r}) - \bar{\omega}(\mathbf{r})) \cdot \mathbf{K}_0$ does not contribute to the pseudomagnetic field. Therefore, the value of the pseudomagnetic field is given by

$$\mathbf{B} = \nabla \times \mathbf{A}(\mathbf{r}), \tag{25}$$

which is exactly the same pseudomagnetic field that appears in other derivations [20,39–41]. Note that, the inclusion of the local rotations tensor $\bar{\omega}(\mathbf{r})$ was necessary to demonstrate the physical irrelevance of the $\mathbf{K}_0$-dependent pseudovector potential.

On the other hand, the complex gauge field $\boldsymbol{\Gamma}$ is owing to a position-dependent Fermi velocity and its presence guarantees the hermiticity of the Hamiltonian (20). Unlike $\mathbf{A}$, $\boldsymbol{\Gamma}$ is a purely imaginary. Thus $\boldsymbol{\Gamma}$ cannot be interpreted as a gauge field and will not give rise to Landau levels in the density of states [39]. However, it may have other physical consequences, such as pseudospin precession, i.e., electronic transitions between the two sublattices [39]. At present, the experimental signatures of such complex gauge field $\boldsymbol{\Gamma}$ are open questions.

3.1. Inclusion of out-of-plane deformations

It is worth mentioning that a second check can be made to Eq. (20) by adapting an independent approach developed by Volovik and Zubkov in Ref. [44] for out-of-plane deformations. Volovik et al. [44] found a similar Hamiltonian, but they used a parametrization thought for curved graphene, where the in-plane coordinates of atoms are identical to their coordinates in the unperturbed honeycomb lattice. The reason is that they were mainly interested in a differential geometry interpretation. Here we used the reference laboratory frame, which is more suitable to compare with experiments, because one must use this frame to describe the interaction with external probes or fields [39]. However, once the equations of Volovik and Zubkov are written in the reference laboratory frame, Eq. (20) for in-plane deformations can be recovered.

Likewise, one can take advantage of both approaches and to write a generalized effective Dirac Hamiltonian. For this end, in β-dependent terms of Eq. (20) one must replace the strain tensor $\bar{\epsilon}$ with the generalized strain tensor

$$\tilde{\epsilon}_{ij} = \frac{1}{2}\left(\frac{\partial u_i}{\partial r_j} + \frac{\partial u_j}{\partial r_i} + \frac{\partial h}{\partial r_i}\frac{\partial h}{\partial r_j}\right)$$
$$= \bar{\epsilon}_{ij} + \frac{1}{2}\frac{\partial h}{\partial r_i}\frac{\partial h}{\partial r_j}, \tag{26}$$

where $\mathbf{u}(\mathbf{r})$ and $h(\mathbf{r})$ are in- and out-of-plane displacements respectively. Thus, finally, the generalized effective Dirac Hamiltonian can be written as

$$H = -i\hbar\boldsymbol{\sigma} \cdot \bar{\mathbf{v}}(\mathbf{r}) \cdot \nabla - \hbar v_F \boldsymbol{\sigma} \cdot \mathbf{A} - \hbar v_F \boldsymbol{\sigma} \cdot \boldsymbol{\Gamma}, \tag{27}$$

where now the generalized position-dependent Fermi velocity tensor $\bar{\boldsymbol{v}}(\boldsymbol{r})$ results

$$\bar{\boldsymbol{v}}(\boldsymbol{r}) = v_F\big(\bar{\boldsymbol{I}} + \bar{\boldsymbol{\epsilon}}(\boldsymbol{r}) - \beta\tilde{\boldsymbol{\epsilon}}(\boldsymbol{r})\big), \tag{28}$$

with the corresponding complex vector field,

$$\Gamma_i = \frac{i}{2v_F}\frac{\partial \bar{v}_{ij}(\boldsymbol{r})}{\partial r_j} = \frac{i}{2}\frac{\partial \bar{\epsilon}_{ij}(\boldsymbol{r})}{\partial r_j} - \frac{i\beta}{2}\frac{\partial \tilde{\epsilon}_{ij}(\boldsymbol{r})}{\partial r_j}, \tag{29}$$

whereas the pseudovector potential $\boldsymbol{A}$ is given by

$$A_x = \frac{\beta}{2a}(\tilde{\epsilon}_{xx} - \tilde{\epsilon}_{yy}), \quad A_y = -\frac{\beta}{2a}(2\tilde{\epsilon}_{xy}). \tag{30}$$

A simple exploration shows that our generalized Hamiltonian (27) reproduces our Hamiltonian for in-plane deformations (Eq. (20)) as well as the equations of Volovik and Zubkov [44], for out-of-plane displacements. Note that, we ignored the term $\big(\bar{\boldsymbol{I}} - \bar{\boldsymbol{\epsilon}}(\boldsymbol{r}) + \bar{\boldsymbol{\omega}}(\boldsymbol{r})\big) \cdot \boldsymbol{K}_0$ due to its demonstrated irrelevance. Consequently, the generalized Hamiltonian (27) describes the particular case of a uniform strain which resolves an inconsistency of previous effective Hamiltonians.

3.2. Effects of position-dependent Fermi velocity on the spinor wavefunction

Finally, let us now consider the effects of a position-dependent Fermi velocity tensor on the spinor wavefunction of charge carriers. For this purpose, we consider the case of an out-of-plane deformation along the x axis given by $h(x)$. Then from Eq. (26) it follows that the generalized strain tensor is,

$$\tilde{\epsilon}_{xx}(x) = \frac{1}{2}(\partial_x h(x))^2 \equiv f(x)/\beta, \quad \tilde{\epsilon}_{yy} = \tilde{\epsilon}_{xy} = 0, \tag{31}$$

thus, one immediately obtains that $\boldsymbol{A} = (f(x)/(2a), 0)$, whereas

$$\bar{\boldsymbol{v}}(x) = v_F\begin{pmatrix} 1 - f(x) & 0 \\ 0 & 1 \end{pmatrix}, \quad \boldsymbol{\Gamma} = (-if'(x)/2, 0). \tag{32}$$

Taking into consideration that the resulting pseudomagnetic field is zero ($B = \partial_x A_y - \partial_y A_x$), from Eq. (27) one can write the corresponding stationary Dirac equation for the spinor wavefunction Ψ as

$$\big(-i(1 - f(x))\partial_x - \partial_y + if'(x)/2\big)\psi_2 = \varepsilon\psi_1,$$
$$\big(-i(1 - f(x))\partial_x + \partial_y + if'(x)/2\big)\psi_1 = \varepsilon\psi_2, \tag{33}$$

where the parameter ε is defined as $\varepsilon \equiv E/(\hbar v_F)$, and E is the energy. If now one supposes that the spinor wavefunction is of the form $\Psi = \exp(ik_y y)\Phi(x)$ then the following differential equation system is obtained,

$$\big((1 - f(x))\partial_x + k_y - f'(x)/2\big)\phi_2 = i\varepsilon\phi_1,$$
$$\big((1 - f(x))\partial_x - k_y - f'(x)/2\big)\phi_1 = i\varepsilon\phi_2. \tag{34}$$

In order to recover the case of flat graphene in the appropriate limit one can cast the following ansatz:

$$\Phi(x) = \exp\bigg[\int^x \frac{ik_x + f'(\tilde{x})/2}{1 - f(\tilde{x})}d\tilde{x}\bigg]\begin{pmatrix} c_1 \\ c_2 \end{pmatrix}, \tag{35}$$

where c_1 and c_2 are constants. Consequently, the differential system (34) becomes the algebraic system

$$(ik_x + k_y)c_2 = i\varepsilon c_1,$$
$$(ik_x + k_y)c_1 = i\varepsilon c_2, \tag{36}$$

which has infinite solutions if $\varepsilon = \pm(k_x^2 + k_y^2)^{1/2}$. Therefore, finally we find that the stationary Dirac equation (33) has as solution the spinor wavefunction

$$\Psi(\boldsymbol{r}) = A\exp\bigg[ik_y y + \int^x \frac{ik_x + f'(\tilde{x})/2}{1 - f(\tilde{x})}d\tilde{x}\bigg]\begin{pmatrix} 1 \\ se^{i\theta} \end{pmatrix}, \tag{37}$$

where $e^{i\theta} = (k_x + ik_y)/|\varepsilon|$, A is a normalization constant and $s = \pm 1$ denotes the conduction band and valence bands, respectively.

A remarkable result follows from our solution (37):

$$|\Psi|^2 \sim (1 - f(x))^{-1} \tag{38}$$

i.e. a position-dependent Fermi velocity induces an inhomogeneity in the carrier probability density. For example, in the interesting case of a flexural mode given by $h(x) = h_0\cos(Gx)$, from Eq. (38) one get $|\Psi|^2 \sim (1 - \tilde{h}\sin^2(Gx))^{-1}$, where $\tilde{h} = \beta h_0^2 G^2/2$. So that, the carrier probability density is minimum at the valleys and at the crests of the flexural mode. To end, let us point out that our findings can be easily extended to the case of an in-plane deformation (along the x) replacing β by $\beta - 1$.

4. Conclusions

In this work we revisited the effective Dirac Hamiltonian for graphene under a uniform strain, starting from a tight-binding description. We simultaneously considered three fundamental strain-induced contributions: *the changes in the nearest-neighbor hopping parameters, the reciprocal lattice deformation and the true shift of the Dirac point.* In particular, the Dirac point did not coincide with the high-symmetry points of the strained reciprocal lattice. A detailed discussion about this last strain-induced effect demonstrates its relevance to obtain the appropriate Fermi velocity. Finally, we presented a generalized effective Dirac Hamiltonian for the case of a nonuniform deformations. This new Hamiltonian reproduces the case of uniform strain in the corresponding limit, which was a missing issue in previous approaches. Within the approach carried out, the strain-induced pseudomagnetic fields were obtained owing to the floating character of the Dirac point $\boldsymbol{K}_D(\boldsymbol{r})$, whereas complex gauge fields appeared as a consequence of a position-dependent Fermi velocity. Our expression (28) for the generalized position-dependent Fermi velocity tensor is the main result in this paper. Also, we found closed analytical solutions for the spinor wavefunctions in cases of practical interest on which the Fermi velocity depends on the position.

Acknowledgements

Appendix A

In this section, the details of the calculations to derive the effective Hamiltonian around $\boldsymbol{K}_0$ are presented. Substituting Eqs. (10) and (11) into Eq. (9) we get

$$H_{\boldsymbol{K}_0} \simeq -t\sum_{n=1}^{3}(1 - \frac{\beta}{a^2}\boldsymbol{\delta}_n \cdot \bar{\boldsymbol{\epsilon}} \cdot \boldsymbol{\delta}_n)(i\frac{\boldsymbol{\sigma} \cdot \boldsymbol{\delta}_n}{a}\sigma_z)$$
$$\times (1 + i\sigma_z\boldsymbol{q} \cdot (\bar{\boldsymbol{I}} + \bar{\boldsymbol{\epsilon}}) \cdot \boldsymbol{\delta}_n)(1 + i\sigma_z\boldsymbol{K}_0 \cdot \bar{\boldsymbol{\epsilon}} \cdot \boldsymbol{\delta}_n),$$

and expanding to first order in strain, H_{K_0} can be written as

$$
H_{K_0} \simeq -t \sum_{n=1}^{3} \left(i \frac{\boldsymbol{\sigma} \cdot \boldsymbol{\delta}_n}{a} \sigma_z \right) \left(1 + i\sigma_z \boldsymbol{q} \cdot (\bar{\boldsymbol{I}} + \bar{\boldsymbol{\epsilon}}) \cdot \boldsymbol{\delta}_n \right.
$$
$$
- \frac{\beta}{a^2} \boldsymbol{\delta}_n \cdot \bar{\boldsymbol{\epsilon}} \cdot \boldsymbol{\delta}_n - \frac{\beta}{a^2} \boldsymbol{\delta}_n \cdot \bar{\boldsymbol{\epsilon}} \cdot \boldsymbol{\delta}_n (i\sigma_z \boldsymbol{q} \cdot \boldsymbol{\delta}_n)
$$
$$
\left. + i\sigma_z \boldsymbol{K}_0 \cdot \bar{\boldsymbol{\epsilon}} \cdot \boldsymbol{\delta}_n - (\boldsymbol{K}_0 \cdot \bar{\boldsymbol{\epsilon}} \cdot \boldsymbol{\delta}_n)(\boldsymbol{q} \cdot \boldsymbol{\delta}_n) \right). \tag{A.1}
$$

Now we collect the contribution of each term of this expression,

$$
-t \sum_{n=1}^{3} \left(i \frac{\boldsymbol{\sigma} \cdot \boldsymbol{\delta}_n}{a} \sigma_z \right) = 0, \tag{A.2}
$$

$$
-t \sum_{n=1}^{3} \left(i \frac{\boldsymbol{\sigma} \cdot \boldsymbol{\delta}_n}{a} \sigma_z \right) (i\sigma_z \boldsymbol{q} \cdot (\bar{\boldsymbol{I}} + \bar{\boldsymbol{\epsilon}}) \cdot \boldsymbol{\delta}_n)
$$
$$
= \hbar v_F \boldsymbol{\sigma} \cdot (\bar{\boldsymbol{I}} + \bar{\boldsymbol{\epsilon}}) \cdot \boldsymbol{q}, \tag{A.3}
$$

$$
t \sum_{n=1}^{3} \left(i \frac{\boldsymbol{\sigma} \cdot \boldsymbol{\delta}_n}{a} \sigma_z \right) \left(\frac{\beta}{a^2} \boldsymbol{\delta}_n \cdot \bar{\boldsymbol{\epsilon}} \cdot \boldsymbol{\delta}_n \right) = -\hbar v_F \boldsymbol{\sigma} \cdot \boldsymbol{A}, \tag{A.4}
$$

$$
t \sum_{n=1}^{3} \left(i \frac{\boldsymbol{\sigma} \cdot \boldsymbol{\delta}_n}{a} \sigma_z \right) \left(\frac{\beta}{a^2} \boldsymbol{\delta}_n \cdot \bar{\boldsymbol{\epsilon}} \cdot \boldsymbol{\delta}_n \right) (i\sigma_z \boldsymbol{q} \cdot \boldsymbol{\delta}_n)
$$
$$
= -\hbar v_F \frac{\beta}{4} \boldsymbol{\sigma} \cdot (2\bar{\boldsymbol{\epsilon}} + \mathrm{Tr}(\bar{\boldsymbol{\epsilon}})\bar{\boldsymbol{I}}) \cdot \boldsymbol{q}, \tag{A.5}
$$

$$
-t \sum_{n=1}^{3} \left(i \frac{\boldsymbol{\sigma} \cdot \boldsymbol{\delta}_n}{a} \sigma_z \right) (i\sigma_z \boldsymbol{K}_0 \cdot \bar{\boldsymbol{\epsilon}} \cdot \boldsymbol{\delta}_n) = \hbar v_F \boldsymbol{\sigma} \cdot \bar{\boldsymbol{\epsilon}} \cdot \boldsymbol{K}_0, \tag{A.6}
$$

$$
t \sum_{n=1}^{3} \left(i \frac{\boldsymbol{\sigma} \cdot \boldsymbol{\delta}_n}{a} \sigma_z \right) (\boldsymbol{K}_0 \cdot \bar{\boldsymbol{\epsilon}} \cdot \boldsymbol{\delta}_n)(\boldsymbol{q} \cdot \boldsymbol{\delta}_n)
$$
$$
= \hbar v_F \boldsymbol{\sigma} \cdot (\frac{a}{2} \boldsymbol{K}_0 \cdot \bar{\boldsymbol{\epsilon}} \cdot \boldsymbol{\sigma}') \cdot \boldsymbol{q}, \tag{A.7}
$$

where $\boldsymbol{\sigma}' = (-\sigma_z, \sigma_x)$ and the $\boldsymbol{A}$ vector is given by Eq. (1) if the x axis is selected parallel to the zigzag direction of the graphene lattice. Finally, taking into account the contribution of each term in Eq. (A.1), given by Eqs. (A.2)–(A.7), the effective Hamiltonian around K_0 has the form of our Eq. (12).

Appendix B

In this section, we include the local rotations in the problem of strained graphene. Note that, under an atomic displacement field $\boldsymbol{u}(\boldsymbol{r})$, the strained nearest-neighbor vectors are given approximately by [38]

$$
\boldsymbol{\delta}_n' \simeq (\bar{\boldsymbol{I}} + \nabla \boldsymbol{u}) \cdot \boldsymbol{\delta}_n, \tag{B.1}
$$

where $\nabla \boldsymbol{u}$ is the displacement gradient tensor:

$$
[\nabla \boldsymbol{u}]_{ij} = \frac{\partial u_i}{\partial r_j} = \frac{1}{2} \left(\frac{\partial u_i}{\partial r_j} + \frac{\partial u_j}{\partial r_i} \right) + \frac{1}{2} \left(\frac{\partial u_i}{\partial r_j} - \frac{\partial u_j}{\partial r_i} \right)
$$
$$
= \bar{\epsilon}_{ij}(\boldsymbol{r}) + \bar{\omega}_{ij}(\boldsymbol{r}), \tag{B.2}
$$

with $\bar{\boldsymbol{\omega}}(\boldsymbol{r})$ being the rotation tensor, which is antisymmetric. A position-dependent rotation tensor $\bar{\boldsymbol{\omega}}(\boldsymbol{r})$ describes the local rotations associated to the displacement field, while if $\bar{\boldsymbol{\omega}}$ is independent on the position, it represents a lattice global rotation which does not have physical implications.

Unlike the strained nearest-neighbor vectors, the three nearest-neighbor hopping parameters t_n' do not dependent on the $\bar{\boldsymbol{\omega}}(\boldsymbol{r})$ tensor,

$$
t_n' \simeq t \left(1 - \frac{\beta}{a^2} \boldsymbol{\delta}_n \cdot \nabla \boldsymbol{u} \cdot \boldsymbol{\delta}_n \right)
$$
$$
\simeq t \left(1 - \frac{\beta}{a^2} \boldsymbol{\delta}_n \cdot \bar{\boldsymbol{\epsilon}}(\boldsymbol{r}) \cdot \boldsymbol{\delta}_n \right), \tag{B.3}
$$

which is an expected result since the rotations do not affect the module of the nearest-neighbor vectors. Thus, one should expect that the $\bar{\boldsymbol{\omega}}(\boldsymbol{r})$ tensor only appears in β-independent terms, i.e., in terms of purely geometric origin.

For our purpose to include the local rotations, let us start with the Hamiltonian of strained graphene in $\boldsymbol{k}$-momentum space [40],

$$
H = -\sum_{n=1}^{3} t_n' \begin{pmatrix} 0 & e^{-i\boldsymbol{k} \cdot (\bar{\boldsymbol{I}} + \nabla \boldsymbol{u}) \cdot \boldsymbol{\delta}_n} \\ e^{i\boldsymbol{k} \cdot (\bar{\boldsymbol{I}} + \nabla \boldsymbol{u}) \cdot \boldsymbol{\delta}_n} & 0 \end{pmatrix}, \tag{B.4}
$$

where $\bar{\boldsymbol{\epsilon}}$ and $\bar{\boldsymbol{\omega}}$ are considered position-independent. In order to obtain the effective Dirac Hamiltonian one must consider momentum close to the Dirac point, $\boldsymbol{k} = \boldsymbol{K}_D + \boldsymbol{q}$. In this case $\boldsymbol{K}_D$ can be casted as

$$
\boldsymbol{K}_D = \left[(\bar{\boldsymbol{I}} + \nabla \boldsymbol{u})^\top \right]^{-1} \cdot (\boldsymbol{K}_0 + \boldsymbol{A})
$$
$$
\simeq (\bar{\boldsymbol{I}} - \bar{\boldsymbol{\epsilon}} + \bar{\boldsymbol{\omega}}) \cdot \boldsymbol{K}_0 + \boldsymbol{A}, \tag{B.5}
$$

which is a generalization of Eq. (13). Substituting Eq. (B.5) into Eq. (B.4) and consistently expanding to first order in strain and $\boldsymbol{q}$ results in,

$$
H = -\sum_{n=1}^{3} t_n' \begin{pmatrix} 0 & e^{-i(\boldsymbol{K}_0 \cdot \boldsymbol{\delta}_n + \boldsymbol{q} \cdot (\bar{\boldsymbol{I}} + \nabla \boldsymbol{u}) \cdot \boldsymbol{\delta}_n + \boldsymbol{A} \cdot \boldsymbol{\delta}_n)} \\ e^{i(\boldsymbol{K}_0 \cdot \boldsymbol{\delta}_n + \boldsymbol{q} \cdot (\bar{\boldsymbol{I}} + \nabla \boldsymbol{u}) \cdot \boldsymbol{\delta}_n + \boldsymbol{A} \cdot \boldsymbol{\delta}_n)} & 0 \end{pmatrix}
$$
$$
= -\sum_{n=1}^{3} t_n' \begin{pmatrix} 0 & e^{-i\boldsymbol{K}_0 \cdot \boldsymbol{\delta}_n} \\ e^{i\boldsymbol{K}_0 \cdot \boldsymbol{\delta}_n} & 0 \end{pmatrix}
$$
$$
\times (1 + i\sigma_z \boldsymbol{q} \cdot (\bar{\boldsymbol{I}} + \nabla \boldsymbol{u}) \cdot \boldsymbol{\delta}_n)(1 + i\sigma_z \boldsymbol{A} \cdot \boldsymbol{\delta}_n). \tag{B.6}
$$

Using once again the identity (10) and replacing t_n' with the expression (B.3) the Hamiltonian (B.6) becomes

$$
H = -t \sum_{n=1}^{3} \left(i \frac{\boldsymbol{\sigma} \cdot \boldsymbol{\delta}_n}{a} \sigma_z \right) \left(1 + i\sigma_z \boldsymbol{q} \cdot (\bar{\boldsymbol{I}} + \nabla \boldsymbol{u}) \cdot \boldsymbol{\delta}_n \right.
$$
$$
- \frac{\beta}{a^2} \boldsymbol{\delta}_n \cdot \bar{\boldsymbol{\epsilon}} \cdot \boldsymbol{\delta}_n (i\sigma_z \boldsymbol{q} \cdot \boldsymbol{\delta}_n) - (\boldsymbol{A} \cdot \boldsymbol{\delta}_n)(\boldsymbol{q} \cdot \boldsymbol{\delta}_n)
$$
$$
\left. - \frac{\beta}{a^2} \boldsymbol{\delta}_n \cdot \bar{\boldsymbol{\epsilon}} \cdot \boldsymbol{\delta}_n + i\sigma_z \boldsymbol{A} \cdot \boldsymbol{\delta}_n \right). \tag{B.7}
$$

The contribution of each term in the last equation is given by Eqs. (A.2), (A.4), (A.5) and

$$
-t \sum_{n=1}^{3} \left(i \frac{\boldsymbol{\sigma} \cdot \boldsymbol{\delta}_n}{a} \sigma_z \right) (i\sigma_z \boldsymbol{q} \cdot (\bar{\boldsymbol{I}} + \nabla \boldsymbol{u}) \cdot \boldsymbol{\delta}_n)
$$
$$
= -t \sum_{n=1}^{3} \left(i \frac{\boldsymbol{\sigma} \cdot \boldsymbol{\delta}_n}{a} \sigma_z \right) (i\sigma_z \boldsymbol{q}^* \cdot \boldsymbol{\delta}_n)
$$
$$
= \hbar v_F \boldsymbol{\sigma} \cdot \boldsymbol{q}^*, \text{ with } \boldsymbol{q}^* = (\bar{\boldsymbol{I}} + \nabla \boldsymbol{u}^\top) \cdot \boldsymbol{q}
$$
$$
= \hbar v_F \boldsymbol{\sigma} \cdot (\bar{\boldsymbol{I}} + \nabla \boldsymbol{u}^\top) \cdot \boldsymbol{q}, \tag{B.8}
$$

$$
t \sum_{n=1}^{3} \left(i \frac{\boldsymbol{\sigma} \cdot \boldsymbol{\delta}_n}{a} \sigma_z \right) (\boldsymbol{A} \cdot \boldsymbol{\delta}_n)(\boldsymbol{q} \cdot \boldsymbol{\delta}_n)
$$
$$
= -\hbar v_F \frac{\beta}{4} \boldsymbol{\sigma} \cdot (2\bar{\boldsymbol{\epsilon}} - \mathrm{Tr}(\bar{\boldsymbol{\epsilon}})\bar{\boldsymbol{I}}) \cdot \boldsymbol{q}, \tag{B.9}
$$

$$
-t \sum_{n=1}^{3} \left(i \frac{\boldsymbol{\sigma} \cdot \boldsymbol{\delta}_n}{a} \sigma_z \right) (i\sigma_z \boldsymbol{A} \cdot \boldsymbol{\delta}_n) = \hbar v_F \boldsymbol{\sigma} \cdot \boldsymbol{A}, \tag{B.10}
$$

where it is worth mentioning that the contributions of the last two terms in Eq. (B.7), Eqs. (A.4) and (B.10), cancel.

After looking the contributions of each term, Eq. (B.7) can be written as

$$H = \hbar v_F \boldsymbol{\sigma} \cdot (\bar{\boldsymbol{I}} + \nabla \boldsymbol{u}^\top - \beta \bar{\boldsymbol{\epsilon}}) \cdot \boldsymbol{q}, \tag{B.11}$$

where $\nabla \boldsymbol{u}^\top = \bar{\boldsymbol{\epsilon}} - \bar{\boldsymbol{\omega}}$. Hamiltonian (B.11) can be considered as the generalization of Eq. (14).

Now to extend Eq. (B.11) to the case of a nonuniform strain we assume that $\bar{\boldsymbol{\epsilon}}(\boldsymbol{r})$ and $\bar{\boldsymbol{\omega}}(\boldsymbol{r})$ are position-dependent and pass to real space by means of the rule [44]

$$\bar{v}_{ij} q_k \to \bar{v}_{ij}(\boldsymbol{r}) \left(-i \frac{\partial}{\partial r_k} - K_k^D(\boldsymbol{r}) \right) - \frac{i}{2} \frac{\partial \bar{v}_{ij}(\boldsymbol{r})}{\partial r_k}. \tag{B.12}$$

In consequence, we obtain that the effective Dirac Hamiltonian for nonuniform in-plane strain is given by

$$H = \hbar \boldsymbol{\sigma} \cdot \bar{\boldsymbol{v}}(\boldsymbol{r}) \cdot (-i\nabla - \boldsymbol{K}_D(\boldsymbol{r})) - \hbar v_F \boldsymbol{\sigma} \cdot \boldsymbol{\Gamma}, \tag{B.13}$$

where

$$\bar{\boldsymbol{v}}(\boldsymbol{r}) = v_F (\bar{\boldsymbol{I}} + \bar{\boldsymbol{\epsilon}}(\boldsymbol{r}) - \bar{\boldsymbol{\omega}}(\boldsymbol{r}) - \beta \bar{\boldsymbol{\epsilon}}(\boldsymbol{r})), \tag{B.14}$$

$$\boldsymbol{K}_D(\boldsymbol{r}) = (\bar{\boldsymbol{I}} - \bar{\boldsymbol{\epsilon}}(\boldsymbol{r}) + \bar{\boldsymbol{\omega}}(\boldsymbol{r})) \cdot \boldsymbol{K}_0 + \boldsymbol{A}(\boldsymbol{r}), \tag{B.15}$$

and

$$\Gamma_i = \frac{i}{2 v_F} \frac{\partial \bar{v}_{ij}(\boldsymbol{r})}{\partial r_j} = \frac{i(1-\beta)}{2} \frac{\partial \bar{\epsilon}_{ij}(\boldsymbol{r})}{\partial r_j} - \frac{i}{2} \frac{\partial \bar{\omega}_{ij}(\boldsymbol{r})}{\partial r_j}, \tag{B.16}$$

with an implicit sum over repeated indices. Finally, we remove the dependence on $\bar{\boldsymbol{\omega}}$ from Eqs. (B.14) and (B.16) carrying out the following local rotation of the pseudospinor

$$\psi \to \exp(\frac{i}{2} \bar{\omega}_{xy} \sigma_3) \psi \simeq \psi + \frac{i}{2} \bar{\omega}_{xy} \sigma_3 \psi, \tag{B.17}$$

and as a consequence, Eq. (B.13) takes the form of our Eq. (20).

References

[1] K.S. Novoselov, et al., Science 306 (2004) 666.
[2] A.K. Geim, Science 324 (2009) 1530.
[3] K.S. Novoselov, Rev. Mod. Phys. 83 (Aug 2011) 837, http://link.aps.org/doi/10.1103/RevModPhys.83.837.
[4] A.H. Castro Neto, F. Guinea, N.M.R. Peres, K.S. Novoselov, A.K. Geim, Rev. Mod. Phys. 81 (Jan 2009) 109, http://link.aps.org/doi/10.1103/RevModPhys.81.109.
[5] M.A.H. Vozmediano, M.I. Katsnelson, F. Guinea, Phys. Rep. (ISSN 0370-1573) 496 (2010) 109, http://www.sciencedirect.com/science/article/pii/S0370157310001729.
[6] F. Guinea, Solid State Commun. (ISSN 0038-1098) 152 (2012) 1437, http://www.sciencedirect.com/science/article/pii/S0038109812002256.
[7] D. Zhan, J. Yan, L. Lai, Z. Ni, L. Liu, Z. Shen, Adv. Mater. (ISSN 1521-4095) 24 (2012) 4055, http://dx.doi.org/10.1002/adma.201200011.
[8] C. Lee, X. Wei, J.W. Kysar, J. Hone, Science 321 (2008) 385.
[9] V.M. Pereira, A.H. Castro Neto, N.M.R. Peres, Phys. Rev. B 80 (Jul 2009) 045401, http://link.aps.org/doi/10.1103/PhysRevB.80.045401.
[10] G. Cocco, E. Cadelano, L. Colombo, Phys. Rev. B 81 (Jun 2010) 241412, http://link.aps.org/doi/10.1103/PhysRevB.81.241412.
[11] M.O. Goerbig, J.-N. Fuchs, G. Montambaux, F. Piéchon, Phys. Rev. B 78 (Jul 2008) 045415, http://link.aps.org/doi/10.1103/PhysRevB.78.045415.
[12] R. de Gail, J.-N. Fuchs, M. Goerbig, F. Piéchon, G. Montambaux, Physica B, Condens. Matter (ISSN 0921-4526) 407 (2012) 1948, http://www.sciencedirect.com/science/article/pii/S0921452612000774.
[13] V.M. Pereira, A.H. Castro Neto, Phys. Rev. Lett. 103 (Jul 2009) 046801, http://link.aps.org/doi/10.1103/PhysRevLett.103.046801.
[14] T. Low, Y. Jiang, M. Katsnelson, F. Guinea, Nano Lett. 12 (2012) 850, http://pubs.acs.org/doi/abs/10.1021/nl2038985.
[15] Y. Jiang, T. Low, K. Chang, M.I. Katsnelson, F. Guinea, Phys. Rev. Lett. 110 (Jan 2013) 046601, http://link.aps.org/doi/10.1103/PhysRevLett.110.046601.
[16] D.A. Gradinar, M. Mucha-Kruczyński, H. Schomerus, V.I. Fal'ko, Phys. Rev. Lett. 110 (Jun 2013) 266801, http://link.aps.org/doi/10.1103/PhysRevLett.110.266801.
[17] H. Hung Nguyen, V. Viet Nguyen, P. Dollfus, Nanotechnology 25 (2014) 165201, http://stacks.iop.org/0957-4484/25/i=16/a=165201.
[18] A. Cortijo, M.A.H. Vozmediano, Europhys. Lett. 77 (2007) 47002, http://stacks.iop.org/0295-5075/77/i=4/a=47002.
[19] M.A.H. Vozmediano, F. de Juan, A. Cortijo, J. Phys. Conf. Ser. 129 (2008) 012001, http://stacks.iop.org/1742-6596/129/i=1/a=012001.
[20] F. de Juan, M. Sturla, M.A.H. Vozmediano, Phys. Rev. Lett. 108 (May 2012) 227205, http://link.aps.org/doi/10.1103/PhysRevLett.108.227205.
[21] J.L. Mañes, Phys. Rev. B 76 (Jul 2007) 045430, http://link.aps.org/doi/10.1103/PhysRevB.76.045430.
[22] R. Winkler, U. Zülicke, Phys. Rev. B 82 (Dec 2010) 245313, http://link.aps.org/doi/10.1103/PhysRevB.82.245313.
[23] T.L. Linnik, J. Phys. Condens. Matter 24 (2012) 205302, http://stacks.iop.org/0953-8984/24/i=20/a=205302.
[24] J.L. Mañes, F. de Juan, M. Sturla, M.A.H. Vozmediano, Phys. Rev. B 88 (Oct 2013) 155405, http://link.aps.org/doi/10.1103/PhysRevB.88.155405.
[25] J.V. Sloan, A.A.P. Sanjuan, Z. Wang, C. Horvath, S. Barraza-Lopez, Phys. Rev. B 87 (Apr 2013) 155436, http://link.aps.org/doi/10.1103/PhysRevB.87.155436.
[26] S. Barraza-Lopez, A.A. Pacheco Sanjuan, Z. Wang, M. Vanević, Solid State Commun. 166 (Jul 2013) 70–75.
[27] A.A. Pacheco Sanjuan, M. Mehboudi, E.O. Harriss, H. Terrones, S. Barraza-Lopez, ACS Nano 8 (2014) 1136, http://pubs.acs.org/doi/abs/10.1021/nn406532z.
[28] A.A. Pacheco Sanjuan, Z. Wang, H. Pour Imani, M. Vanević, S. Barraza-Lopez, Phys. Rev. B 89 (Mar 2014) 121403, http://link.aps.org/doi/10.1103/PhysRevB.89.121403.
[29] G.G. Naumis, P. Roman-Taboada, Phys. Rev. B 89 (Jun 2014) 241404, http://link.aps.org/doi/10.1103/PhysRevB.89.241404.
[30] F. Guinea, M.I. Katsnelson, A.K. Geim, Nat. Phys. 6 (2010) 30.
[31] Z. Qi, D.A. Bahamon, V.M. Pereira, H.S. Park, D.K. Campbell, A.H.C. Neto, Nano Lett. 13 (2013) 2692, http://pubs.acs.org/doi/abs/10.1021/nl400872q.
[32] M. Neek-Amal, F.M. Peeters, Phys. Rev. B 85 (May 2012) 195446, http://link.aps.org/doi/10.1103/PhysRevB.85.195446.
[33] R. Carrillo-Bastos, D. Faria, A. Latgé, F. Mireles, N. Sandler, Phys. Rev. B 90 (Jul 2014) 041411, http://link.aps.org/doi/10.1103/PhysRevB.90.041411.
[34] Z. Qi, A.L. Kitt, H.S. Park, V.M. Pereira, D.K. Campbell, A.H. Castro Neto, Phys. Rev. B 90 (Sep 2014) 125419, http://link.aps.org/doi/10.1103/PhysRevB.90.125419.
[35] N. Levy, S.A. Burke, K.L. Meaker, M. Panlasigui, A. Zettl, F. Guinea, A.H.C. Neto, M.F. Crommie, Science 329 (2010) 544, http://www.sciencemag.org/content/329/5991/544.abstract.
[36] J. Lu, A.C. Neto, K.P. Loh, Nat. Commun. 3 (May 2012) 823, http://dx.doi.org/10.1038/ncomms1818.
[37] A.L. Kitt, V.M. Pereira, A.K. Swan, B.B. Goldberg, Phys. Rev. B 85 (Mar 2012) 115432, http://link.aps.org/doi/10.1103/PhysRevB.85.115432.
[38] A.L. Kitt, V.M. Pereira, A.K. Swan, B.B. Goldberg, Phys. Rev. B 87 (Apr 2013) 159909 (Erratum), http://link.aps.org/doi/10.1103/PhysRevB.87.159909.
[39] F. de Juan, J.L. Mañes, M.A.H. Vozmediano, Phys. Rev. B 87 (Apr 2013) 165131, http://link.aps.org/doi/10.1103/PhysRevB.87.165131.
[40] M.R. Masir, D. Moldovan, F. Peeters, Solid State Commun. (ISSN 0038-1098) 175–176 (2013) 76, http://www.sciencedirect.com/science/article/pii/S0038109813001555.
[41] H.T. Yang, J. Phys. Condens. Matter 23 (2011) 505502, http://stacks.iop.org/0953-8984/23/i=50/a=505502.
[42] M. Oliva-Leyva, G.G. Naumis, Phys. Rev. B 88 (Aug 2013) 085430, http://link.aps.org/doi/10.1103/PhysRevB.88.085430.
[43] M. Zubkov, G. Volovik, arXiv:1308.2249, http://arxiv.org/abs/1308.2249.
[44] G. Volovik, M. Zubkov, Ann. Phys. (ISSN 0003-4916) 340 (2014) 352, http://www.sciencedirect.com/science/article/pii/S0003491613002558.
[45] R.M. Ribeiro, V.M. Pereira, N.M.R. Peres, P.R. Briddon, A.H. Castro Neto, New J. Phys. 11 (2009) 115002, http://stacks.iop.org/1367-2630/11/i=11/a=115002.
[46] C. Bena, G. Montambaux, New J. Phys. 11 (2009) 095003, http://stacks.iop.org/1367-2630/11/i=9/a=095003.
[47] M. Oliva-Leyva, G.G. Naumis, J. Phys. Condens. Matter 26 (2014) 125302, http://stacks.iop.org/0953-8984/26/i=12/a=125302.
[48] M. Oliva-Leyva, G.G. Naumis, J. Phys. Condens. Matter 26 (2014) 279501, http://stacks.iop.org/0953-8984/26/i=27/a=279501.
[49] V.M. Pereira, R.M. Ribeiro, N.M.R. Peres, A.H. Castro Neto, Europhys. Lett. 92 (2010) 67001, http://stacks.iop.org/0295-5075/92/i=6/a=67001.
[50] G.-X. Ni, H.-Z. Yang, W. Ji, S.-J. Baeck, C.-T. Toh, J.-H. Ahn, V.M. Pereira, B. Özyilmaz, Adv. Mater. (ISSN 1521-4095) 26 (2014) 1081, http://dx.doi.org/10.1002/adma.201304156.
[51] M. Oliva-Leyva, G.G. Naumis, 2D Mater. 2 (2015) 025001, http://stacks.iop.org/2053-1583/2/i=2/a=025001.
[52] C.D. Froggatt, H.B. Nielsen, Origin of Symmetry, World Scientific, Singapore, 1991.
[53] G.E. Volovik, The Universe in a Helium Droplet, Clarendon Press, Oxford, 2003.
[54] P. Hořava, Phys. Rev. Lett. 95 (Jun 2005) 016405, http://link.aps.org/doi/10.1103/PhysRevLett.95.016405.
[55] H. Yan, Z.-D. Chu, W. Yan, M. Liu, L. Meng, M. Yang, Y. Fan, J. Wang, R.-F. Dou, Y. Zhang, Z. Liu, J.-C. Nie, L. He, Phys. Rev. B 87 (Feb 2013) 075405, http://link.aps.org/doi/10.1103/PhysRevB.87.075405.
[56] W.-J. Jang, H. Kim, Y.-R. Shin, M. Wang, S.K. Jang, M. Kim, S. Lee, S.-W. Kim, Y.J. Song, S.-J. Kahng, Carbon (ISSN 0008-6223) 74 (2014) 139, http://www.sciencedirect.com/science/article/pii/S0008622314002619.